Uncover Treasures in DCT: Advancing JPEG Quality Enhancement by Exploiting Latent Correlations

Supplementary Material

1. Proof of DCT-domain Upsampling Module Equivalent to Pixel-domain (UMEP)

1.1. Block-based Chroma Upsampling

In the main paper, we proposed a DCT-domain Upsampling Module Equivalent to Pixel-domain (UMEP) that achieves equivalent results to pixel-domain upsampling. In this section, we provide detailed derivations and proofs for this method.

Assume we have an $N \times N$ pixel block $\mathbf{B}_N$. To upsample this block by a factor of 2 into a $2N \times 2N$ pixel block $\mathbf{B}_{2N}$, we can use nearest-neighbor upsampling, which can be efficiently implemented using NumPy broadcasting:

$$\mathbf{B}_{2N} = \mathbf{U}_N \mathbf{B}_N \mathbf{U}_N^\top, \tag{1}$$

where $\mathbf{U}_N$, with shape $(2N, N)$, represents the upsampling matrix:

$$\mathbf{U}_N = \begin{cases} \begin{bmatrix} 1 \\ 1 \end{bmatrix} & \text{if } N = 1, \\ \begin{bmatrix} \mathbf{U}_1 & \cdots & 0 \\ \vdots & \ddots & \vdots \\ 0 & \cdots & \mathbf{U}_1 \end{bmatrix} & \text{if } N > 1. \end{cases} \tag{2}$$

Similarly, we can upsample a DCT block $\hat{\mathbf{B}}_N$ by a factor of 2 as follows:

$$\hat{\mathbf{B}}_{2N} = \mathbf{U}_N \hat{\mathbf{B}}_N \mathbf{U}_N^\top. \tag{3}$$

However, DCT blocks are not suitable for spatial upsampling. These blocks contain spatially decorrelated coefficients, while spatial upsampling methods assume that neighboring values are correlated and change continuously. As a result, direct upsampling of DCT coefficients may result in aliasing and artifacts.[1] The intuitive solution is to first inverse-transform the DCT block back to the pixel domain, upsample the pixel block, and then transform it back to the DCT domain. Unfortunately, this process is computationally expensive.

Now, we aim to derive a DCT-domain upsampling matrix $\hat{\mathbf{U}}_N$ that yields equivalent results to pixel-domain upsampling. Our mathematical goal is to achieve:

$$\hat{\mathbf{B}}_{2N} = \hat{\mathbf{U}}_N \hat{\mathbf{B}}_N \hat{\mathbf{U}}_N^\top, \tag{4}$$

$$= \mathbf{T}_{2N} \mathbf{B}_{2N} \mathbf{T}_{2N}^\top, \tag{5}$$

where $\mathbf{T}_{2N}$ is the 1-D DCT basis matrix of size $2N \times 2N$ [1]. Based on Eq. (1), we replace $\mathbf{B}_{2N}$ in Eq. (5) and obtain:

$$\hat{\mathbf{B}}_{2N} = \mathbf{T}_{2N} \left(\mathbf{U}_N \mathbf{B}_N \mathbf{U}_N^\top \right) \mathbf{T}_{2N}^\top, \tag{6}$$

$$= \left(\mathbf{T}_{2N} \mathbf{U}_N \right) \mathbf{B}_N \left(\mathbf{T}_{2N} \mathbf{U}_N \right)^\top. \tag{7}$$

Combining Eq. (4) and Eq. (7), we have:

$$\hat{\mathbf{U}}_N \hat{\mathbf{B}}_N \hat{\mathbf{U}}_N^\top = \left(\mathbf{T}_{2N} \mathbf{U}_N \right) \mathbf{B}_N \left(\mathbf{T}_{2N} \mathbf{U}_N \right)^\top. \tag{8}$$

Considering $\hat{\mathbf{B}}_N = \mathbf{T}_N \mathbf{B}_N \mathbf{T}_N^\top$ in Eq. (8), we have:

$$\hat{\mathbf{U}}_N \left(\mathbf{T}_N \mathbf{B}_N \mathbf{T}_N^\top \right) \hat{\mathbf{U}}_N^\top = \left(\hat{\mathbf{U}}_N \mathbf{T}_N \right) \mathbf{B}_N \left(\hat{\mathbf{U}}_N \mathbf{T}_N \right)^\top, \tag{9}$$

$$= \left(\mathbf{T}_{2N} \mathbf{U}_N \right) \mathbf{B}_N \left(\mathbf{T}_{2N} \mathbf{U}_N \right)^\top. \tag{10}$$

Therefore, we derive $\hat{\mathbf{U}}_N = \mathbf{T}_{2N} \mathbf{U}_N \mathbf{T}_N^{-1} = \mathbf{T}_{2N} \mathbf{U}_N \mathbf{T}_N^\top$. Note that the DCT basis matrix $\mathbf{T}$ is orthogonal, meaning $\mathbf{T}^{-1} = \mathbf{T}^\top$. As a result, we obtain the ideal DCT-domain upsampling by $\hat{\mathbf{U}}_N$ that yields equivalent results to pixel-domain upsampling by $\mathbf{U}_N$:

$$\hat{\mathbf{B}}_{2N} = \hat{\mathbf{U}}_N \hat{\mathbf{B}}_N \hat{\mathbf{U}}_N^\top, \tag{11}$$

$$= \left(\mathbf{T}_{2N} \mathbf{U}_N \mathbf{T}_N^\top \right) \hat{\mathbf{B}}_N \left(\mathbf{T}_{2N} \mathbf{U}_N \mathbf{T}_N^\top \right)^\top. \tag{12}$$

1.2. Application to JPEG Chroma Upsampling

Ideally, we can upsample each 4×4 DCT block by a DCT-domain upsampling matrix $\hat{\mathbf{U}}_4 = \mathbf{T}_8 \mathbf{U}_4 \mathbf{T}_4^\top$, such that we can achieve equivalent results to pixel-domain upsampling by $\mathbf{U}_4$. However, in JPEG, there exist only 8×8 chroma DCT blocks, which are obtained by combining four neighboring downsampled 4×4 chroma pixel blocks following DCT transformation. To obtain four 4×4 chroma DCT blocks from each 8×8 chroma DCT block, we adopt the sub-block conversion method [2, 3]:

$$\mathbf{H}_2^\top \hat{\mathbf{B}}_8 \mathbf{H}_2 = \begin{bmatrix} \hat{\mathbf{B}}_4^{(0,0)} & \hat{\mathbf{B}}_4^{(0,1)} \\ \hat{\mathbf{B}}_4^{(1,0)} & \hat{\mathbf{B}}_4^{(1,1)} \end{bmatrix}, \tag{13}$$

where $\mathbf{H}_2$ is the sub-block conversion matrix with shape 8×8; $\hat{\mathbf{B}}_4^{(0,0)}$ to $\hat{\mathbf{B}}_4^{(1,1)}$ are the converted 4×4 chroma DCT blocks. Finally, we can apply our DCT-domain upsampling as in Eq. (11) to these converted 4×4 blocks:

$$\hat{\mathbf{B}}_8 = \hat{\mathbf{U}}_4 \hat{\mathbf{B}}_4 \hat{\mathbf{U}}_4^\top. \tag{14}$$

[1] Our ablation study shows that directly upsampling chroma DCT blocks can lead to at least a 0.1 dB PSNR degradation in performance.

Dataset	QF	JPEG	AJQE w/ AR-CNN	AJQE w/ DCAD	AJQE w/ DnCNN	AJQE w/ FBCNN	AJQE w/ ARCRL	QGAC	JDEC
BSDS500	10	23.67	26.83 (+0.38)	26.80 (+0.01)	26.96 (+0.06)	27.45 (+0.12)	**27.58** (+0.28)	26.64	27.04
	20	25.89	29.10 (+0.30)	29.38 (+0.07)	29.41 (+0.09)	29.89 (+0.14)	**30.06** (+0.32)	29.15	29.40
	30	27.28	30.31 (+0.16)	30.70 (+0.01)	30.51 (+0.12)	31.10 (+0.03)	**31.12** (–0.03)	30.41	30.78
	40	28.28	31.17 (+0.13)	31.75 (+0.10)	31.77 (+0.01)	**32.28** (+0.30)	32.23 (+0.24)	31.25	31.76
LIVE-1	10	23.96	26.66 (+0.27)	26.70 (+0.02)	26.78 (–0.06)	27.53 (+0.04)	**27.75** (+0.43)	26.81	26.14
	20	26.27	28.98 (+0.22)	29.25 (+0.01)	29.49 (+0.01)	29.91 (+0.05)	**30.16** (+0.32)	29.05	29.48
	30	27.64	30.18 (+0.06)	30.88 (+0.14)	30.54 (+0.12)	31.22 (+0.03)	**31.27** (+0.07)	30.28	30.82
	40	28.63	31.05 (+0.06)	31.73 (+0.04)	31.96 (+0.14)	32.19 (+0.11)	**32.26** (+0.12)	31.07	31.65
ICB	10	27.66	30.98 (+0.75)	31.09 (+0.28)	31.17 (+0.15)	32.05 (+0.17)	**32.08** (+0.17)	31.68	31.71
	20	30.65	33.58 (+0.43)	33.69 (+0.02)	33.88 (+0.10)	**34.42** (+0.04)	34.41 (+0.08)	34.02	34.21
	30	32.15	34.73 (+0.16)	35.12 (+0.02)	35.08 (+0.29)	**35.82** (+0.10)	35.65 (+0.07)	35.08	35.31
	40	33.23	35.82 (+0.34)	36.13 (+0.08)	36.16 (+0.06)	**36.68** (+0.18)	36.61 (+0.13)	35.85	36.08

Table 1. **PSNR-B (dB) results for color JPEG image quality enhancement.** Performance improvements over the pixel-domain model are shown in parentheses. The best results are boldfaced.

Dataset	QF	JPEG	AJQE w/ AR-CNN	AJQE w/ DCAD	AJQE w/ DnCNN	AJQE w/ FBCNN	AJQE w/ ARCRL	QGAC
SSIM								
BSDS500	10	0.781	0.833 (+.019)	0.835 (+.013)	0.834 (+.009)	0.837 (+.007)	**0.838** (+.002)	0.822
	20	0.856	0.897 (+.018)	0.898 (+.012)	0.897 (+.009)	0.899 (+.008)	**0.900** (+.011)	0.885
	30	0.889	0.920 (+.017)	0.923 (+.009)	0.923 (+.008)	**0.924** (+.007)	**0.924** (+.001)	0.911
	40	0.908	0.938 (+.014)	0.938 (+.009)	0.938 (+.008)	0.939 (+.007)	**0.940** (+.007)	0.926
LIVE-1	10	0.784	0.839 (+.019)	0.842 (+.013)	0.840 (+.008)	0.844 (+.005)	**0.845** (+.004)	0.829
	20	0.856	0.900 (+.019)	0.901 (+.012)	0.900 (+.008)	0.902 (+.006)	**0.903** (+.005)	0.888
	30	0.888	0.921 (+.018)	0.924 (+.009)	0.924 (+.007)	0.925 (+.005)	**0.929** (+.002)	0.913
	40	0.905	0.938 (+.015)	0.939 (+.010)	0.939 (+.008)	0.939 (+.006)	**0.940** (+.009)	0.926
ICB	10	0.863	0.913 (+.012)	0.914 (+.009)	0.914 (+.007)	0.917 (+.006)	**0.918** (+.001)	0.908
	20	0.912	0.943 (+.011)	0.943 (+.008)	0.943 (+.007)	0.943 (+.005)	**0.944** (+.005)	0.936
	30	0.932	0.953 (+.009)	0.955 (+.007)	0.955 (+.006)	**0.956** (+.006)	0.955 (+.001)	0.948
	40	0.943	0.961 (+.008)	0.962 (+.007)	0.962 (+.006)	0.962 (+.005)	**0.963** (+.007)	0.956
Classic-5	10	0.783	0.848 (+.026)	0.852 (+.019)	0.851 (+.011)	0.852 (+.006)	**0.856** (+.008)	0.839
	20	0.850	0.896 (+.024)	0.897 (+.017)	0.896 (+.014)	0.898 (+.012)	**0.899** (+.007)	0.880
	30	0.879	0.914 (+.018)	0.917 (+.016)	0.917 (+.015)	0.918 (+.013)	**0.919** (+.017)	0.900
	40	0.895	0.927 (+.019)	0.928 (+.015)	0.928 (+.007)	0.928 (+.012)	**0.930** (+.006)	0.911
PSNR-B								
BSDS500	10	25.03	28.96 (+0.10)	29.14 (+0.13)	29.20 (+0.08)	29.52 (+0.07)	**29.56** (+0.12)	29.17
	20	27.11	31.32 (+0.30)	31.54 (+0.17)	31.51 (+0.03)	31.81 (+0.13)	**31.86** (+0.19)	31.31
	30	28.48	32.24 (+0.26)	32.97 (+0.18)	32.87 (+0.07)	33.22 (+0.23)	**33.27** (+0.20)	32.54
	40	29.48	33.70 (+0.47)	33.92 (+0.28)	33.90 (+0.16)	34.01 (+0.11)	**34.25** (+0.16)	33.40
LIVE-1	10	25.55	29.11 (+0.25)	29.16 (–0.02)	28.94 (+0.06)	**29.68** (+0.12)	29.63 (+0.13)	29.15
	20	27.70	31.48 (+0.46)	31.51 (+0.09)	31.59 (+0.04)	**31.97** (+0.15)	31.96 (+0.02)	31.26
	30	29.04	32.60 (+0.68)	32.86 (+0.03)	32.95 (+0.08)	33.10 (+0.00)	**33.26** (+0.02)	32.42
	40	30.02	33.70 (+0.51)	33.73 (+0.08)	33.91 (+0.12)	34.13 (+0.16)	**34.17** (+0.04)	33.21
ICB	10	30.21	34.67 (+0.43)	34.73 (+0.10)	34.77 (+0.09)	**35.64** (+0.09)	**35.64** (+0.15)	35.18
	20	33.08	37.50 (+0.57)	37.43 (+0.08)	37.49 (+0.04)	38.01 (+0.04)	**38.08** (+0.14)	37.69
	30	34.66	38.65 (+0.41)	38.91 (+0.09)	38.94 (–0.05)	**39.32** (+0.06)	39.31 (+0.15)	38.95
	40	35.75	39.83 (+0.50)	39.87 (+0.17)	39.88 (+0.03)	40.16 (+0.11)	**40.25** (+0.13)	39.75
Classic-5	10	26.11	30.48 (+0.31)	30.74 (+0.17)	30.63 (+0.13)	**31.15** (+0.03)	31.11 (+0.11)	30.80
	20	28.50	32.71 (+0.34)	32.86 (+0.07)	32.71 (+0.01)	**33.37** (+0.16)	33.29 (+0.14)	32.84
	30	30.02	33.94 (+0.36)	33.92 (+0.03)	34.12 (+0.05)	**34.48** (+0.16)	34.41 (+0.19)	33.95
	40	31.08	34.85 (+0.45)	34.92 (+0.12)	34.60 (+0.81)	35.19 (+0.15)	**35.20** (+0.10)	34.66

Table 2. **SSIM and PSNR-B (dB) results for grayscale JPEG image quality enhancement.** Performance improvements over the pixel-domain model are shown in parentheses. The best results are boldfaced. Note that JDEC does not support grayscale enhancement.

2. Additional Experimental Results

The main paper presents the PSNR and SSIM results for enhanced color JPEG images, as well as the PSNR results for grayscale JPEG images, with QF values ranging from 10 to 40 for both. In this section, we provide the PSNR-B results for color JPEG image quality enhancement in Tab. 1, and the SSIM and PSNR-B results for grayscale JPEG image quality enhancement in Tab. 2.

Consistently, our results show that our DCT-domain models outperform both pixel-domain models and other DCT-domain models in terms of quantitative performance

QF	Metric	DIV2K						BSDS500					
		Y		Cb		Cr		Y		Cb		Cr	
		Pixel	DCT	Pixel	DCT	Pixel	DCT	Pixel	DCT	Pixel	DCT	Pixel	DCT
10	$MI\uparrow$	0.947	0.007	0.978	0.009	0.978	0.008	0.935	0.006	0.989	0.010	0.990	0.008
	$GC\downarrow$	0.053	1.003	0.022	0.998	0.022	0.998	0.065	0.999	0.011	0.999	0.010	0.995
20	$MI\uparrow$	0.946	0.007	0.977	0.008	0.977	0.008	0.927	0.006	0.990	0.009	0.991	0.008
	$GC\downarrow$	0.054	1.002	0.023	0.999	0.023	0.998	0.073	0.999	0.010	0.999	0.009	0.996
30	$MI\uparrow$	0.946	0.007	0.977	0.008	0.977	0.009	0.922	0.006	0.990	0.009	0.991	0.008
	$GC\downarrow$	0.054	1.003	0.023	0.999	0.023	1.000	0.078	0.999	0.010	0.999	0.009	0.996
40	$MI\uparrow$	0.946	0.007	0.976	0.008	0.977	0.008	0.919	0.006	0.990	0.009	0.991	0.008
	$GC\downarrow$	0.054	1.002	0.024	1.000	0.023	0.999	0.081	0.999	0.010	0.999	0.009	0.996
50	$MI\uparrow$	0.945	0.007	0.976	0.008	0.976	0.008	0.915	0.006	0.990	0.009	0.990	0.008
	$GC\downarrow$	0.055	1.003	0.024	0.999	0.024	0.999	0.085	0.999	0.010	0.999	0.010	0.996
60	$MI\uparrow$	0.946	0.007	0.976	0.009	0.975	0.009	0.913	0.006	0.990	0.009	0.990	0.008
	$GC\downarrow$	0.054	1.003	0.024	0.999	0.025	0.999	0.087	0.999	0.010	0.999	0.010	0.996
70	$MI\uparrow$	0.946	0.007	0.975	0.009	0.975	0.008	0.910	0.006	0.990	0.009	0.990	0.008
	$GC\downarrow$	0.054	1.002	0.025	0.999	0.025	0.999	0.090	0.999	0.010	0.999	0.010	0.996
80	$MI\uparrow$	0.946	0.007	0.974	0.008	0.975	0.009	0.907	0.006	0.989	0.009	0.990	0.008
	$GC\downarrow$	0.054	1.002	0.026	0.998	0.025	0.999	0.093	0.999	0.010	0.999	0.010	0.996
90	$MI\uparrow$	0.947	0.007	0.973	0.009	0.973	0.008	0.905	0.006	0.989	0.009	0.989	0.008
	$GC\downarrow$	0.053	1.003	0.027	1.000	0.027	0.999	0.095	0.999	0.011	0.999	0.011	0.996
100	$MI\uparrow$	0.946	0.007	0.971	0.008	0.972	0.008	0.911	0.006	0.988	0.009	0.987	0.008
	$GC\downarrow$	0.054	1.003	0.029	0.999	0.028	0.999	0.089	0.999	0.012	0.999	0.013	0.996

Table 3. **Correlations within pixel values and DCT coefficients with QF ranging 10 to 100 on the DIV2K and BSDS500 datasets.** Note that *MI* ranges from -1 to 1, where values close to 1 and 0 represent strong positive and negligible correlations, respectively. Conversely, *GC* ranges from 0 to 2, where values close to 0 and 1 represent strong positive and negligible correlations, respectively.

for both color and grayscale JPEG image quality enhancement. Specifically, our DCT-domain models demonstrate an average PSNR-B improvement of 0.14 dB over pixel-domain methods and an average improvement of 0.23 dB over other DCT-domain methods for color JPEG image quality enhancement. Moreover, for grayscale JPEG images, our DCT-domain models achieve a 0.17 dB improvement over pixel-domain methods and a 0.26 dB improvement over other DCT-domain models. In conclusion, our method significantly enhances the effectiveness of JPEG image quality enhancement, achieving substantial improvements in all metrics.

3. Additional Finding Results

In the main paper, we highlighted two critical correlations within the DCT coefficients of the luminance components of JPEG images at a QF of 50. This section extends our observations to include both the luminance and chroma components across QF values ranging from 10 to 100. Tab. 3 demonstrates the consistently strong correlations present within pixel values of both luminance and chroma components across all QF values, whereas the DCT coefficients exhibit relatively weaker spatial correlations. Figs. 1 to 20 illustrate the substantial block-based and point-based correlations within DCT coefficients, further reinforcing the consistency of our findings presented in the main paper.

References

[1] N. Ahmed, T. Natarajan, and K.R. Rao. Discrete Cosine Transform. *IEEE Transactions on Computers*, C-23(1):90–93, 1974. 1

[2] Jeongsoo Park and Justin Johnson. Rgb no more: Minimally-decoded jpeg vision transformers. In *Proceedings of the IEEE/CVF Conference on Computer Vision and Pattern Recognition (CVPR)*, pages 22334–22346, 2023. 1

[3] Carlos Salazar and Trac D. Tran. A Complexity Scalable Universal DCT Domain Image Resizing Algorithm. *IEEE Transactions on Circuits and Systems for Video Technology*, 17(4): 495–499, 2007. 1

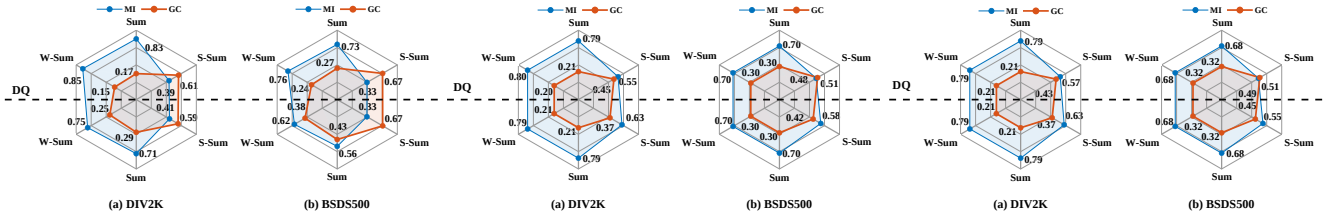

(a) Y (b) Cb (c) Cr

Figure 1. **Block-based correlations using different block-based features on the DIV2K and BSDS500 datasets with QF set to 10.** Upper: DCT blocks are dequantized before calculating feature values. Lower: DCT blocks remain quantized.

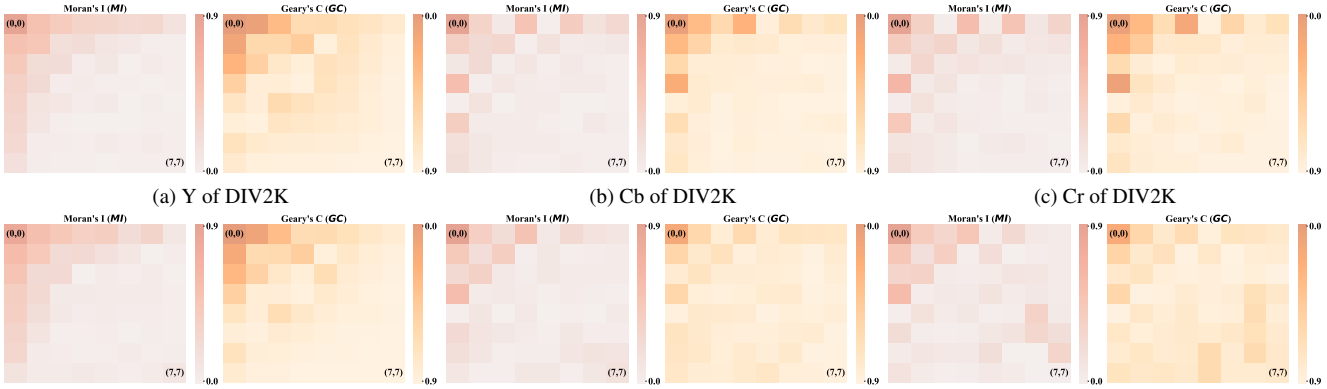

(a) Y of DIV2K (b) Cb of DIV2K (c) Cr of DIV2K

(d) Y of BSDS500 (e) Cb of BSDS500 (f) Cr of BSDS500

Figure 2. **Point-based correlations using coefficient maps on the DIV2K and BSDS500 datasets with QF set to 10.** Note that the intensity of heat maps indicate the strength of the correlations.

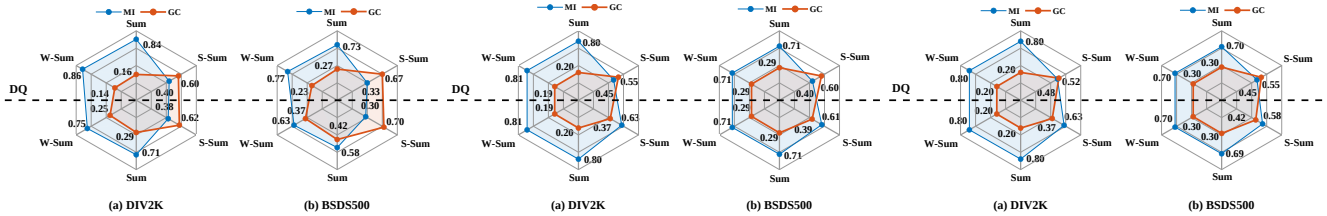

(a) Y (b) Cb (c) Cr

Figure 3. **Block-based correlations using different block-based features on the DIV2K and BSDS500 datasets with QF set to 20.** Upper: DCT blocks are dequantized before calculating feature values. Lower: DCT blocks remain quantized.

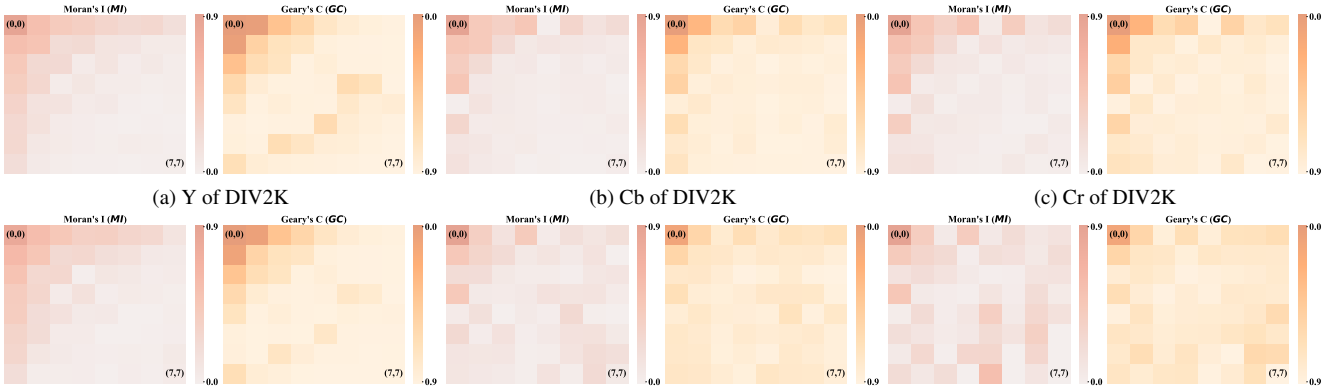

(a) Y of DIV2K (b) Cb of DIV2K (c) Cr of DIV2K

(d) Y of BSDS500 (e) Cb of BSDS500 (f) Cr of BSDS500

Figure 4. **Point-based correlations using coefficient maps on the DIV2K and BSDS500 datasets with QF set to 20.** Note that the intensity of heat maps indicate the strength of the correlations.

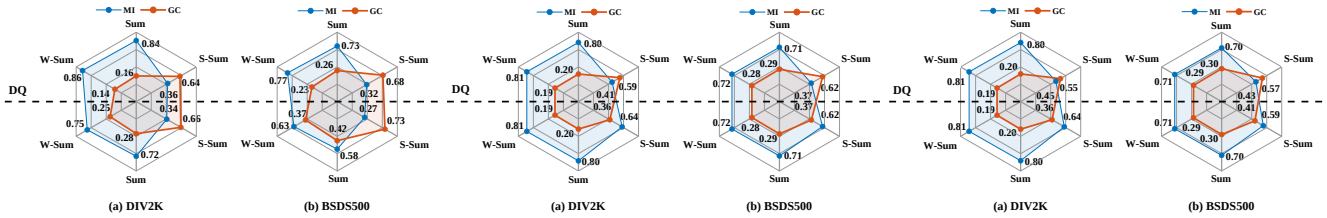

(a) Y (b) Cb (c) Cr

Figure 5. **Block-based correlations using different block-based features on the DIV2K and BSDS500 datasets with QF set to 30.** Upper: DCT blocks are dequantized before calculating feature values. Lower: DCT blocks remain quantized.

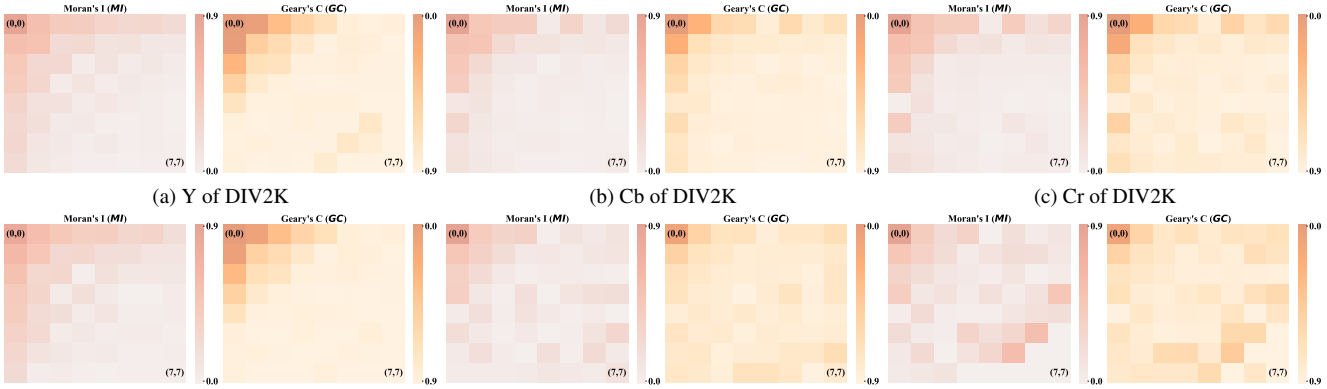

(a) Y of DIV2K (b) Cb of DIV2K (c) Cr of DIV2K

(d) Y of BSDS500 (e) Cb of BSDS500 (f) Cr of BSDS500

Figure 6. **Point-based correlations using coefficient maps on the DIV2K and BSDS500 datasets with QF set to 30.** Note that the intensity of heat maps indicate the strength of the correlations.

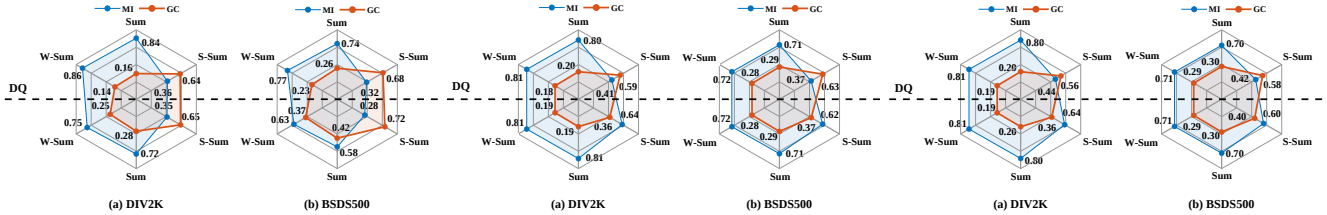

(a) Y (b) Cb (c) Cr

Figure 7. **Block-based correlations using different block-based features on the DIV2K and BSDS500 datasets with QF set to 40.** Upper: DCT blocks are dequantized before calculating feature values. Lower: DCT blocks remain quantized.

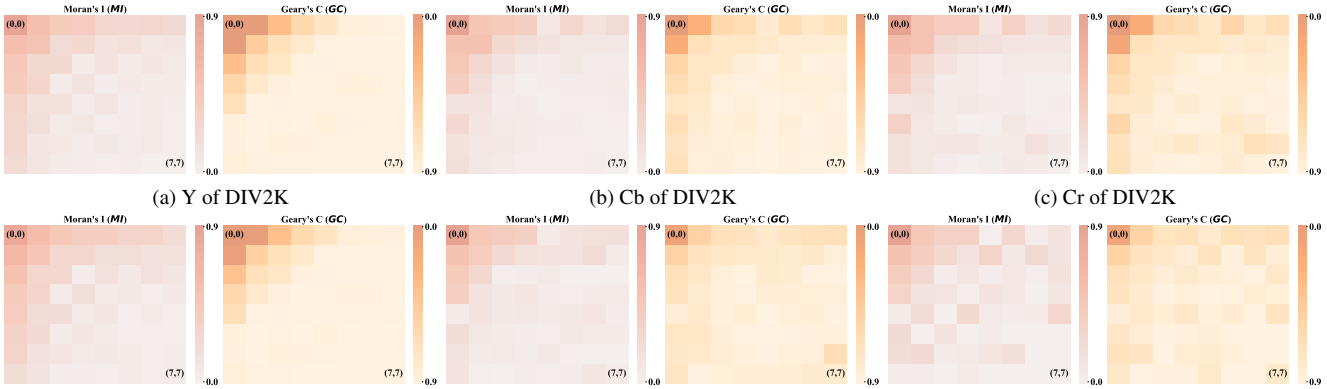

(a) Y of DIV2K (b) Cb of DIV2K (c) Cr of DIV2K

(d) Y of BSDS500 (e) Cb of BSDS500 (f) Cr of BSDS500

Figure 8. **Point-based correlations using coefficient maps on the DIV2K and BSDS500 datasets with QF set to 40.** Note that the intensity of heat maps indicate the strength of the correlations.

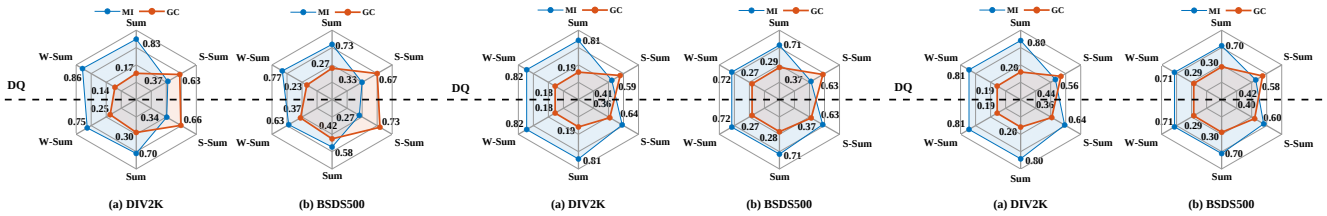

(a) Y (b) Cb (c) Cr

Figure 9. **Block-based correlations using different block-based features on the DIV2K and BSDS500 datasets with QF set to 50.** Upper: DCT blocks are dequantized before calculating feature values. Lower: DCT blocks remain quantized.

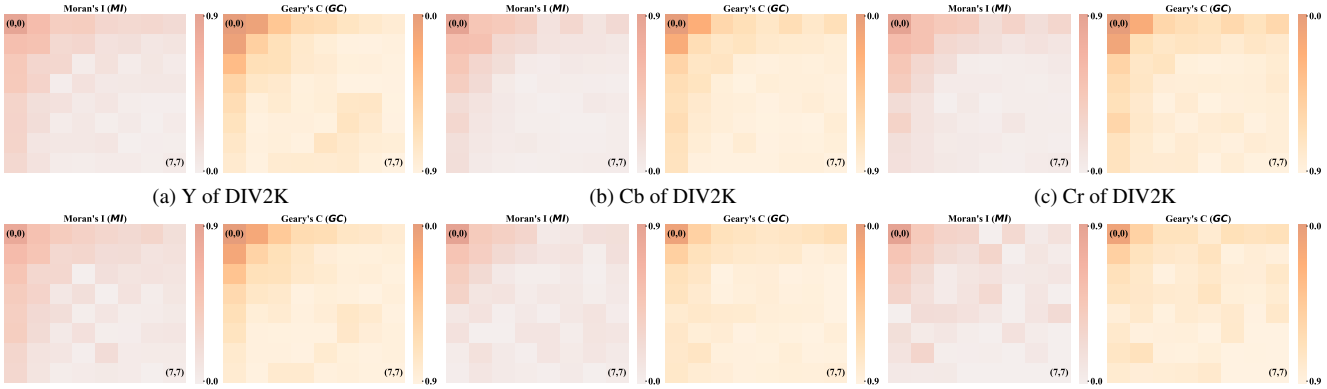

(a) Y of DIV2K (b) Cb of DIV2K (c) Cr of DIV2K

(d) Y of BSDS500 (e) Cb of BSDS500 (f) Cr of BSDS500

Figure 10. **Point-based correlations using coefficient maps on the DIV2K and BSDS500 datasets with QF set to 50.** Note that the intensity of heat maps indicate the strength of the correlations.

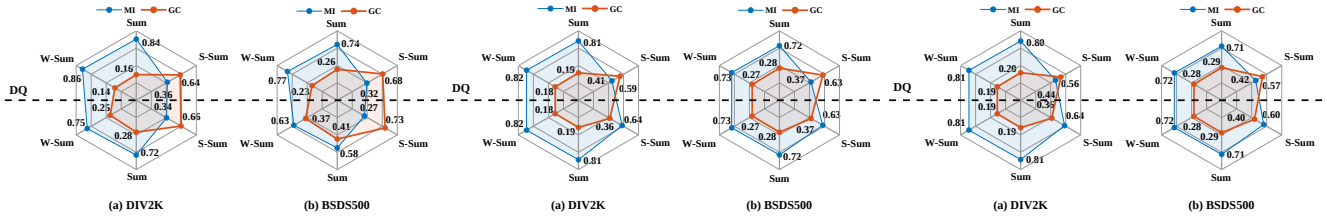

(a) Y (b) Cb (c) Cr

Figure 11. **Block-based correlations using different block-based features on the DIV2K and BSDS500 datasets with QF set to 60.** Upper: DCT blocks are dequantized before calculating feature values. Lower: DCT blocks remain quantized.

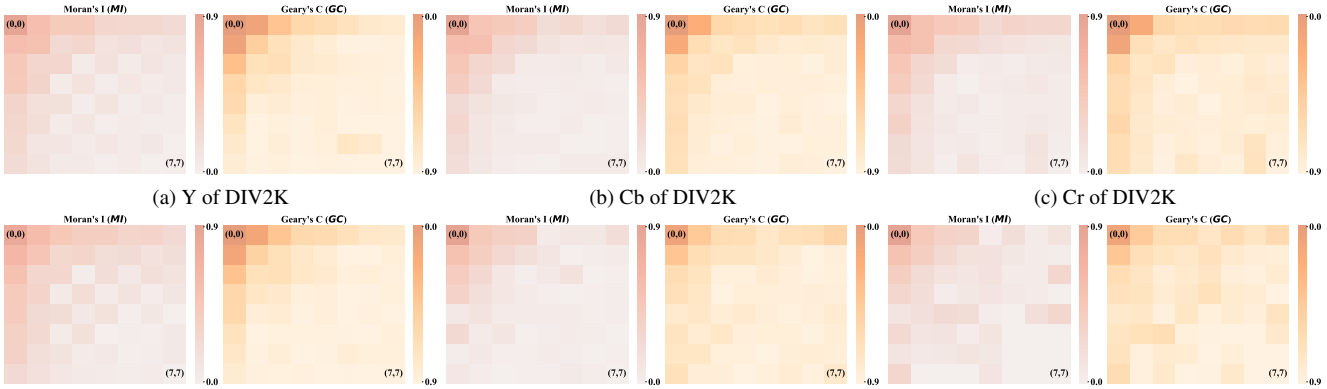

(a) Y of DIV2K (b) Cb of DIV2K (c) Cr of DIV2K

(d) Y of BSDS500 (e) Cb of BSDS500 (f) Cr of BSDS500

Figure 12. **Point-based correlations using coefficient maps on the DIV2K and BSDS500 datasets with QF set to 60.** Note that the intensity of heat maps indicate the strength of the correlations.

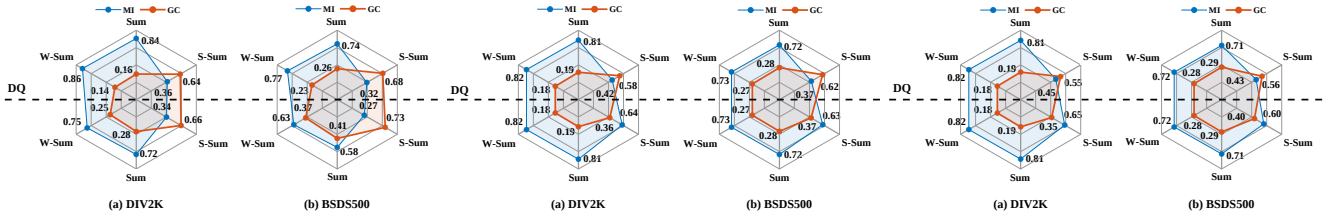

(a) Y (b) Cb (c) Cr

Figure 13. **Block-based correlations using different block-based features on the DIV2K and BSDS500 datasets with QF set to 70.** Upper: DCT blocks are dequantized before calculating feature values. Lower: DCT blocks remain quantized.

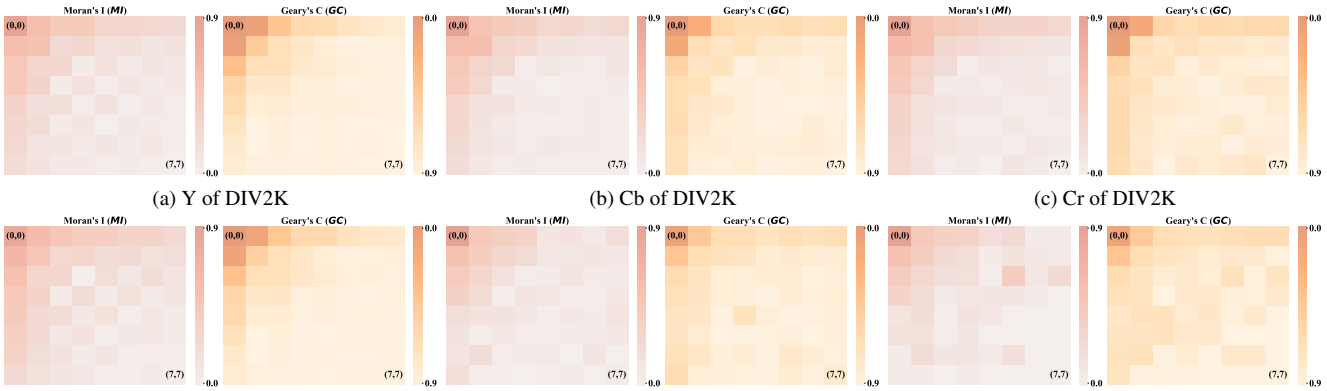

(a) Y of DIV2K (b) Cb of DIV2K (c) Cr of DIV2K

(d) Y of BSDS500 (e) Cb of BSDS500 (f) Cr of BSDS500

Figure 14. **Point-based correlations using coefficient maps on the DIV2K and BSDS500 datasets with QF set to 70.** Note that the intensity of heat maps indicate the strength of the correlations.

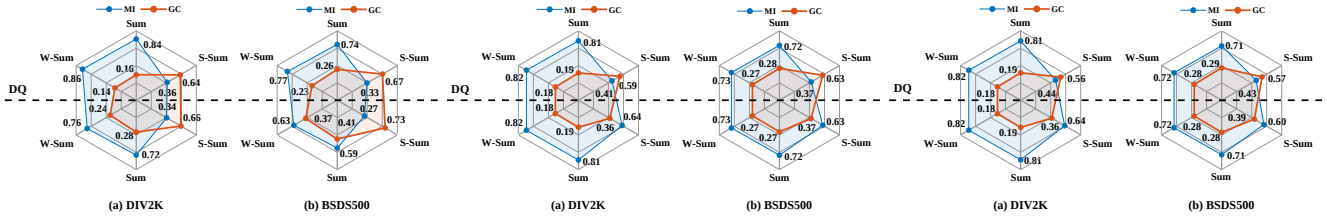

(a) Y (b) Cb (c) Cr

Figure 15. **Block-based correlations using different block-based features on the DIV2K and BSDS500 datasets with QF set to 80.** Upper: DCT blocks are dequantized before calculating feature values. Lower: DCT blocks remain quantized.

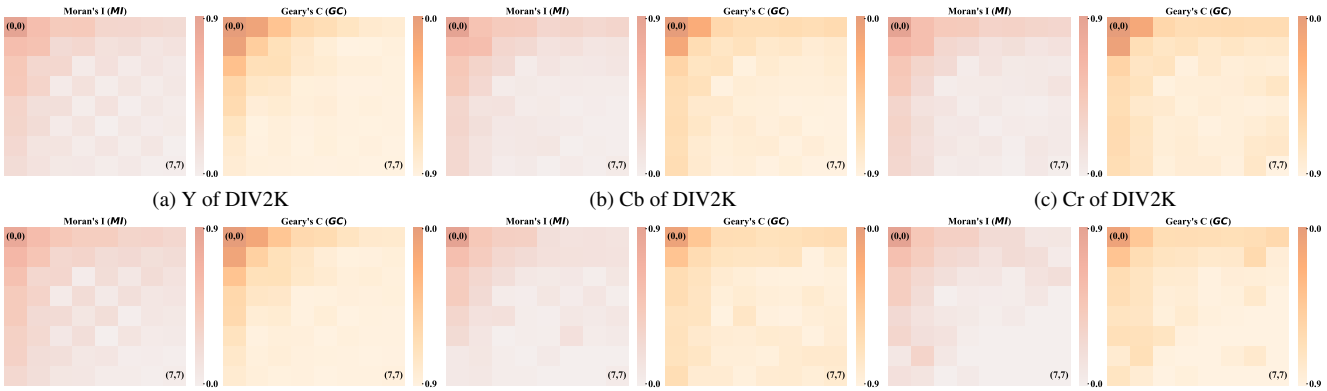

(a) Y of DIV2K (b) Cb of DIV2K (c) Cr of DIV2K

(d) Y of BSDS500 (e) Cb of BSDS500 (f) Cr of BSDS500

Figure 16. **Point-based correlations using coefficient maps on the DIV2K and BSDS500 datasets with QF set to 80.** Note that the intensity of heat maps indicate the strength of the correlations.

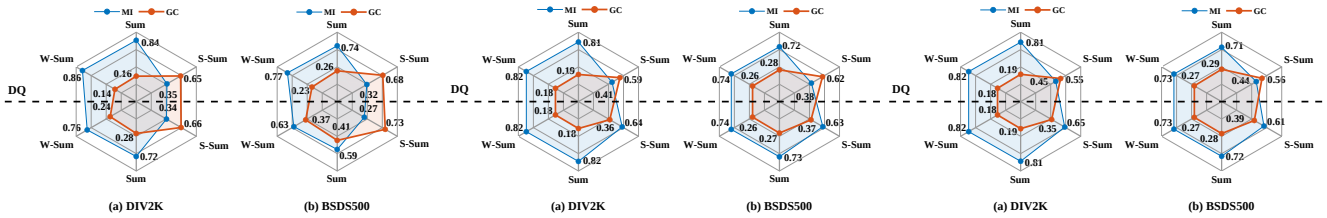

(a) Y (b) Cb (c) Cr

Figure 17. **Block-based correlations using different block-based features on the DIV2K and BSDS500 datasets with QF set to 90.** Upper: DCT blocks are dequantized before calculating feature values. Lower: DCT blocks remain quantized.

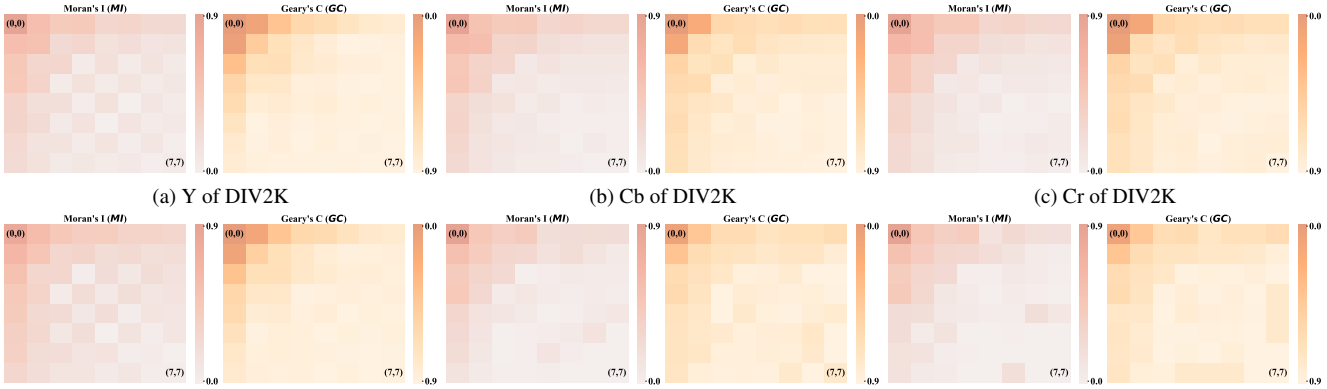

(a) Y of DIV2K (b) Cb of DIV2K (c) Cr of DIV2K

(d) Y of BSDS500 (e) Cb of BSDS500 (f) Cr of BSDS500

Figure 18. **Point-based correlations using coefficient maps on the DIV2K and BSDS500 datasets with QF set to 90.** Note that the intensity of heat maps indicate the strength of the correlations.

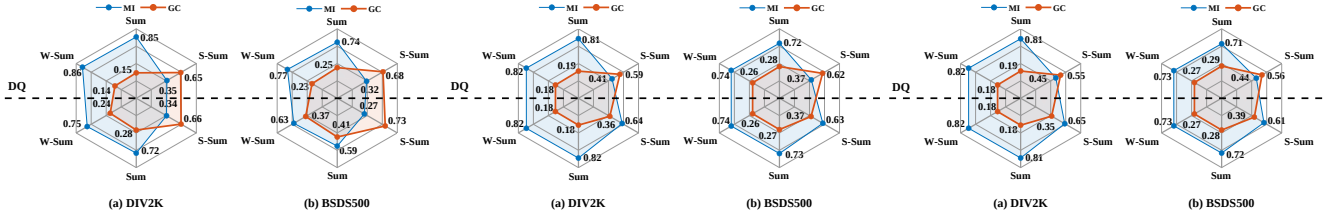

(a) Y (b) Cb (c) Cr

Figure 19. **Block-based correlations using different block-based features on the DIV2K and BSDS500 datasets with QF set to 100.** Upper: DCT blocks are dequantized before calculating feature values. Lower: DCT blocks remain quantized.

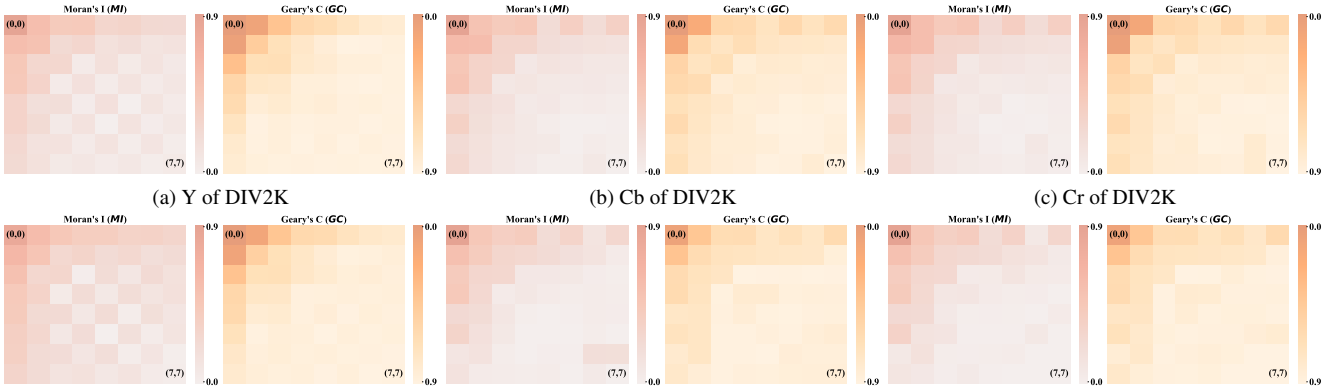

(a) Y of DIV2K (b) Cb of DIV2K (c) Cr of DIV2K

(d) Y of BSDS500 (e) Cb of BSDS500 (f) Cr of BSDS500

Figure 20. **Point-based correlations using coefficient maps on the DIV2K and BSDS500 datasets with QF set to 100.** Note that the intensity of heat maps indicate the strength of the correlations.